Dark and photogenerated ac conductivity in As_2S_3 single crystals

M. Abkowitz, D. F. Blossey, and A. I. Lakatos
Xerox Corporation, 800 Phillips Road, Webster, New York 14580
(Received 17 March 1975)

There has been continuing speculation that the origin of frequency-dependent ac conductivity commonly observed in amorphous insulators may lie in some broad spectrum of relaxation processes specifically characteristic of long-range disorder. However, ac conductivity exhibiting this type of ω^s ($s\sim 1$) behavior is observed in both amorphous and single crystal As_2S_3 as well as in anthracene crystals, suggesting the familiar picture of losses controlled by electronic dissipation in localized states, which need not arise from disorder-induced potential fluctuations but can simply reflect the existence of defects, impurities, and microinterfaces. Combining accompanying b-axis dielectric measurements on As_2S_3 with optical data enables us to estimate for the low-frequency dielectric constants (12.1, 5.9, 10.6) along the a, b, and c axes, respectively. Analysis of photogenerated ac conductivity in As_2S_3 under conditions of bulk illumination leads to an estimated $\mu\tau$ product in the 10^{-8}–10^{-9}-cm^2/V range while comparison with drift-mobility data leads to a nominal estimate of 100 nsec for the recombination lifetime. It is demonstrated that the shape of spectral dependence of photogenerated ac conductivity can vary with ac bias frequency. Finally ac conductance and capacitance in As_2S_3 under illumination with strongly absorbed light are found to exhibit dc bias-field dependence which appears to depend on crystal thickness.

I. INTRODUCTION

In recent years, numerous studies reporting ac conductivity, which exhibits slightly sublinear frequency dependence ($\sigma\propto\omega^s$, $s<1$) have appeared in the literature on noncrystalline solids.[1,2] A principal aim of these studies was elucidation of a presumed localized-state density in the mobility gap. Carriers executing phonon-assisted hops among these states would give rise to a fluctuating polarization characterized by a broad distribution of relaxation times.[1] In the absence of stronger dissipative mechanisms, this process would ultimately control dielectric loss. Under these circumstances, ac measurements provide information about the nature and density of hopping sites. ac experiments in noncrystalline solids all manifest features common with those observed in doped compensated crystalline silicon[3,4] at temperatures for which the residual (impurity) conductivity is known to arise from carriers hopping in a manifold of well-characterized localized states. On the other hand, observation of ac conductivity exhibiting ω^s-type frequency dependence has proved so pervasive in a wide class of noncrystalline solids that questions concerning its origin continue to be raised.[5,6] The linear-heat-capacity anomaly[7] reported in representative amorphous solids and attributed to the absence of long-range order, at least serves to raise the question whether the origin of frequency-dependent conductivity lies in some broad spectrum of relaxation processes, also specifically characteristic of long-range disorder and not necessarily electronic in origin. In fact, Strom *et al.*[8] interpret the microwave and farinfrared absorption, which is observed to be much larger in some amorphous materials than in their crystalline counterparts, as arising specifically from a disorder-induced coupling of radiation to a density of low-frequency Debye modes. There is then the interesting implication that this process might extend to lower frequencies. Austin and Garbett[9] had earlier suggested a similar mechanism arising with relaxation of the selection rules governing phonon absorption in their interpretation of ac conductivity in crystalline and amorphous materials at radio frequencies.

We thought it would be useful to present at this point results of some dark ac-conductivity measurements principally on single crystals of As_2S_3 (orpiment), which together with comparative measurements on anthracene appear in Sec. 3 A. Both these crystals are room-temperature insulators, and like many amorphous insulators, both exhibit the familiar sublinear frequency-dependent ac conductivity at room temperature. Comparison of dark ac conductivity in amorphous[10] and crystalline As_2S_3 thus provides us with no compelling reason to invoke an underlying density of states, specifically associated with long-range positional disorder as an explanation of the origin of frequency-dependent conductivity in the amorphous phase. On the contrary, we suggest that a picture of bulk losses associated with displacement of charge in localized electronic states, which exist to varying extent in all solids containing a population of defects, impurities, or internal microinterfaces remains more plausible as a general rationalization for this behavior.

Orpiment (As_2S_3) is attractive in its own right, not only because of its relationship to an important class of amorphous solids but because it is a two-

dimensional network crystal characterized by large bonding anisotropy. In the remainder of this paper, we therefore discuss dielectric properties and some aspects of photoconductivity measured in As_2S_3 crystals by ac techniques. In Sec. III B low-frequency b-axis dielectric measurements are compared with optical data to complete a dielectric characterization of crystalline As_2S_3, and results are tabulated. Photogenerated ac conductivity observed under illumination with weakly absorbed light is analyzed in Sec. III C 1. In Sec. III C 2 we discuss the case when light is strongly absorbed, emphasizing the behavior of the photogenerated ac conductance and capacitance under superimposed dc bias. Section III D summarizes our results.

II. EXPERIMENTAL

A. Samples

The thin As_2S_3 platelets used in these measurements were cleaved from natural orpiment crystals obtained from Wards Scientific. Most of the measurements were made in a sandwich configuration with electrolytic contacts on the ac faces. Conductivity was therefore measured along the b crystal axis. Cleaved platelets were initially selected by examination under cross polarizers to minimize thickness nonuniformity over the electroded area. Microscopic examination showed some separation along internal cleavage planes. Samples were preselected to minimize such microscopically visible damage. During the experiments samples were often remounted in the electrolytic cell. This additional mechanical handling had no detectable influence on the measurements. Sample thickness was determined by an interferometric technique.

Anthracene crystals were grown from a supersaturated solution of Prinz quality grade anthracene (Princeton organics) in methanol. Measurements were carried out along the normal to the extended face in the as-grown crystal, which is parallel to both the a and b crystal axes. The dielectric constant is anisotropic, and only the b axis of the susceptibility tensor is coincident with the crystalline b axis. Thickness of anthracene sample crystals was estimated from capacitance measurements using an average dielectric constant[11a] of 3. In the ac plane, the dielectric constant varied between 2.45 and 4.80. It is 3.24 in the b direction.[11b]

B. Electrical measurements

ac measurements were made using a conventional transformer ratio-arm bridge operating in a three-terminal configuration. A tee arrangement permitted simultaneous application of dc bias. Either a conventional tuned amplifier or a two-channel lock-in amplifier was used as a null detector. I-V measurements were carried out in parallel with the ac measurements as required, using an electrometer. Current equilibrium was established within a few seconds. Temperature variation was carried out in a programmable environmental test chamber with temperature stability better than 0.5 °C. A quartz fiber optic bundle provided optical access. Exciting radiation was provided either by a GE OXN 1000-W tungsten lamp operating through a Leiss double prism monochromator or by a 300-W tungsten halogen lamp operating through appropriate filters directly coupled to the fiber optics bundle. Photon flux was measured using a calibrated EG & G type SGD-100-A photodiode.

III. RESULTS AND DISCUSSION

A. Dark conductivity

Figure 1 shows the $\sigma \propto \omega^s$ frequency dependence of dark ac conductivity in a 14-μm-thick platelet of As_2S_3 measured at room temperature. The insert on the upper part of the figure shows the electrolytic sample cell used in making these measurements. The liquid contacts were transparent aqueous NaCl solutions. Results were insensitive to the type of salt used (NaI, KI, NaCl). Windows were quartz, and platinum wires were used to make electrical contact to the liquids as indicated.

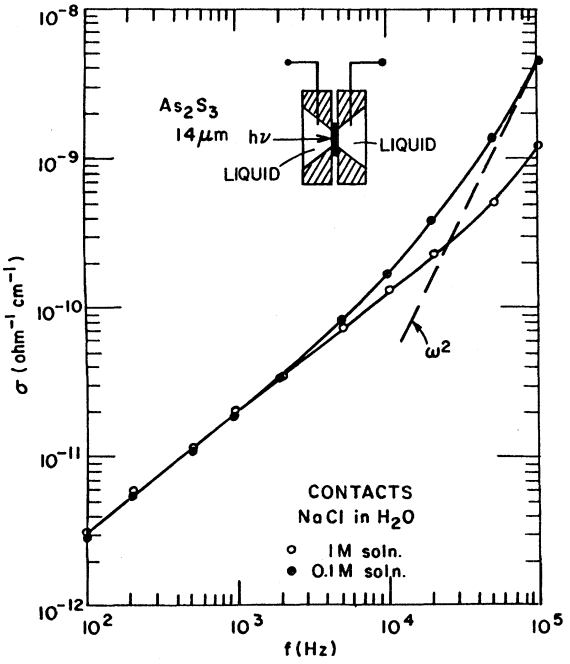

FIG. 1. ac conductivity vs frequency for a 14 μm As_2S_3 single crystal measured in the electrolytic cell configuration depicted. Open circles are results using 1-M saline solution while full circles are results using 0.1-M saline solution. $T = 294$ °K. ac bias is 100-mV rms.

We encountered no difficulty in making repeatable temperature-dependence measurements from just above the solution freezing point to about 350°K. Samples measured with electrolytic contacts could be removed, dried, and remounted numerous times without affecting the results. Typical reproducibility of successive measurements on a given crystal is indicated by the open and closed circles below 3 kHz. Deviation from $S = 0.85 \pm 0.10$ above 3 kHz directly illustrates the influence on these ac measurements of varying contact sheet resistance. The open circles represent measurements made with the higher-conductivity 1-M NaCl solution, the solid circles represent measurements made using 0.1-M solutions. Onset of an asymptotic approach of the conductivity to ω^2 dependence occurs first for the higher-resistance contact. An equivalent circuit analysis in which the contact is represented as a series resistor does predict a transition from sublinear to ω^2 dependence at a characteristic frequency, which depends on combined effects of sample resistance capacitance and contact sheet resistance.[10] The use of electrolytic contacts enables us to demonstrate this experimentally, on a given sample *in situ*. The use of the effective dc-conductivity values determined from the linear I-V curves measured in the electrolytic cell suggests that frequency dependence of ac conductivity persists down to the 10^{-2}-Hz range. It should, however, be noted that linear I-V curves in highly insulating solids are not *prima facie* evidence of Ohmic conduction.[12]

Figure 2 shows the frequency dependence of dark ac conductivity in a 20-μm-thick anthracene platelet measured at room temperature. This sample was also measured in an electrolytic cell using aqueous 1 M NaCl solution contacts. After one set of measurements, the sample was removed and then remounted, a second set of similar contacts formed, and the measurements repeated. Results of the initial and second set of measurements on this crystal are represented by the open and solid circles, respectively. The data on this plot are based on a capacitatively determined thickness using a dielectric constant of 3.0. Typical contact area was 0.044 cm^2. The bowing at high frequencies is again a manifestation of contact resistance, which becomes more severe as molarity of the solution contacts is lowered.

The repeatability of ac measurements on any given sample of As_2S_3 or anthracene is a useful benchmark against which measurements on a relatively large number of As_2S_3 crystal platelets can be compared. Figure 1, which contains data collected on a 14-μm sample, represents ac conductivity versus frequency close to the mean values obtained in measurements on ten samples. Although each sample exhibited characteristic ω^s-type frequency dependence with $s \sim 0.85$, the maximum sample-to-sample scatter observed in comparing respective measurements was just under a decade in conductivity at all frequencies. This scatter was at least a factor of 5 larger than that observed in the anthracene measurements and larger by about the same factor than the scatter observed when comparing ac-conductivity measurements on a sampling of amorphous chalcogenide films[13] prepared under controlled conditions. There appeared to be no clear correlation between apparent ac conductivity and sample thickness, and no spurious variation in dielectric constant. While we did not attempt any extensive correlation of ac conductivity with drift mobility measurements on As_2S_3 crystals, the time-of-flight technique[14] directly indicated large sample-to-sample variation in trap population. In fact, in preliminary experiments the spread in lifetimes ($\Delta\tau \sim 10^2$) among representative samples was such that in some cases a current transient could not be observed at all. A much smaller variation in trap population as inferred from sample-to-sample variation in deep trapping lifetime was observed in the anthracene crystals. The parallel measurements on anthracene were motivated principally by our interest in documenting frequency-dependent conductivity in another insulating crystal, but

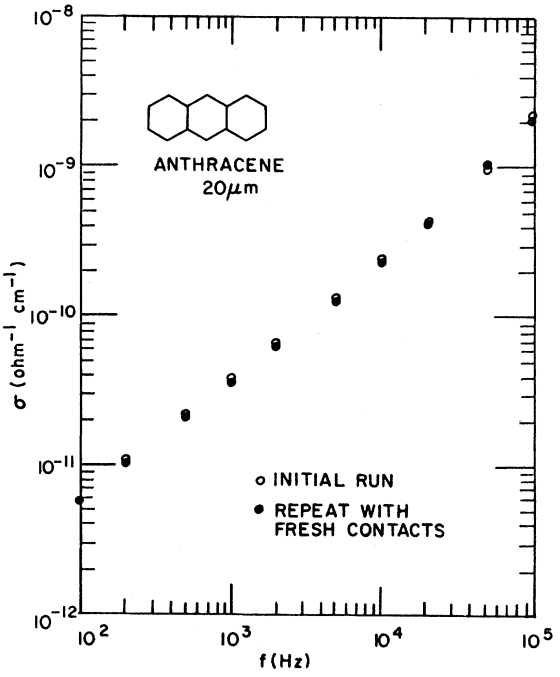

FIG. 2. ac conductivity vs frequency for a 20-μm anthracene crystal. Open circles represent initial data while full circles are repeat measurements following sample removal and remount $T = 294$°K. Bias 100-mV rms. 1-M saline solution.

one devoid of the layer structure unique to As_2S_3 and its isomorphs. A crystal with layer structure could in principle exhibit apparent frequency-dependent conductivity quite apart from that associated with any microscopic dissipation processes. Multiple-layer dielectric structures with their numerous interfaces are often represented in terms of an equivalent circuit consisting of a series string of *RC* tanks. Associated with this representation could be a broad distribution of relaxation times, namely the set of *RC* time constants associated with the respective layer interfacial relaxations. If, however, the origin of the frequency dependence observed in the ac conductivity of As_2S_3 is interfacial relaxation, then one might expect some manifestation of this in the frequency dependence of photogenerated ac conductivity as well. Such effects have been observed via photogenerated ac conductivity in studies comparing polycrystalline compactions and films with the corresponding single-crystal photoconductor.[15] In Sec. III C we show that no such effects are evident in the frequency dependence of our photogenerated ac-conductivity data in As_2S_3, that is, the photogenerated incremental conductivity is observed to be frequency independent.

The dark ac conductivity in As_2S_3 is of comparable magnitude and exhibits the same frequency dependence in both its crystalline and amorphous forms. The underlying microscopic dissipation mechanism appears to be common to a wide class of insulating solids. The interpretation of this loss mechanism in terms of electronic hopping is made by analogy with ac conductivity in doped Si and Ge crystals measured at temperatures for which impurity conduction is the residual transport process. In this case, it was critical to the interpretation that the density of hopping sites could be both independently determined and caused to vary over several orders of magnitude by adjusting doping levels and compensation ratios.[3] Resolution of questions about the origin of frequency-dependent dark conductivity in amorphous insulators depends largely on identifying model materials in which the density of hopping sites, whatever their origin, can be varied significantly.

B. Dielectric properties of As_2S_3

Low crystal symmetry and large bonding anisotropy are responsible for the highly anisotropic optical and low-frequency dielectric properties of As_2S_3. Optical properties for light polarized along the layer (*ac*) plane crystal axes are well established. Recently, the optical constants normal to the layer plane along the *b* axis have also been reported. The most accurate estimates of optical dielectric constants in the layer plane are provided by the interferometric measurements of Evans and Young.[16] Infrared and optical dielectric constants are reported by Taylor *et al.*,[17] and have also been reported by Zallen *et al.*[18] The optical constants reported by Zallen *et al.* are higher, and those reported by Taylor *et al.* are lower, than the corresponding interferometric data. Nevertheless both Zallen *et al.* and Taylor *et al.* agree on the infrared contribution to the dielectric constant $\Delta\epsilon = \epsilon_{ac} - \epsilon_{\infty}$. It appears then, that the incremental change in dielectric constant on going from the visible to the infrared can be determined accurately from reflectivity data. The high-frequency dielectric constants along the *a*, *b*, and *c* axes are ($\epsilon_{\infty} = 8.82, \ldots, 7.02$) from Evans and Young,[16] ($\epsilon_{\infty} = 7.43,\ 4.67,\ 6.20$) from Taylor *et al.*,[17] and ($\epsilon_{\infty} = 11.0, \cdots, 7.3$) from Zallen *et al.*[18] From the infrared measurements, the associated incremental contribution to the dielectric constants are ($\Delta\epsilon_{\infty} = 3.3,\ 0.2,\ 3.5$).[17,18] On the basis of audio frequency measurements carried out on about fifteen selected crystal samples whose respective thicknesses were interferrometrically determined to better than 1%, we estimate

$$\epsilon_b = 5.9 \pm 0.2 .$$

The estimated 6% error reflects uncertainty in the active contact area when using the liquid cell. The best composite estimate of the over-all dielectric properties of crystalline As_2S_3 is summarized in Table I. The asterisk indicates calculated entries. Included for comparison are the corresponding data for amorphous As_2S_3.

C. Photogenerated ac conductivity

1. Bulk illumination

Figure 3 shows the dark ac conductivity and the ac conductivity under 2.66-eV illumination for a 14-μm As_2S_3 crystal when the photon flux is 10^{15} photons $cm^{-2}\,sec^{-1}$. The insert shows the edge absorption along the crystalline *a* and *c* axes.[19] Excitation energy was chosen to insure uniformity of bulk penetration while simultaneously maximizing the measured photoeffect. In the lower figure, we illustrate the frequency independence of the sample capacitance under illumination represented as a

TABLE I. As_2S_3 Dielectric constants.

	Crystal			Amorphous
	a	*b*	*c*	
ϵ_{∞}	8.8	5.7*	7.0	5.8
$\Delta\epsilon$	3.3	0.2	3.6	2.1
ϵ_0	12.1*	5.9	10.6*	7.9

*Calculated values

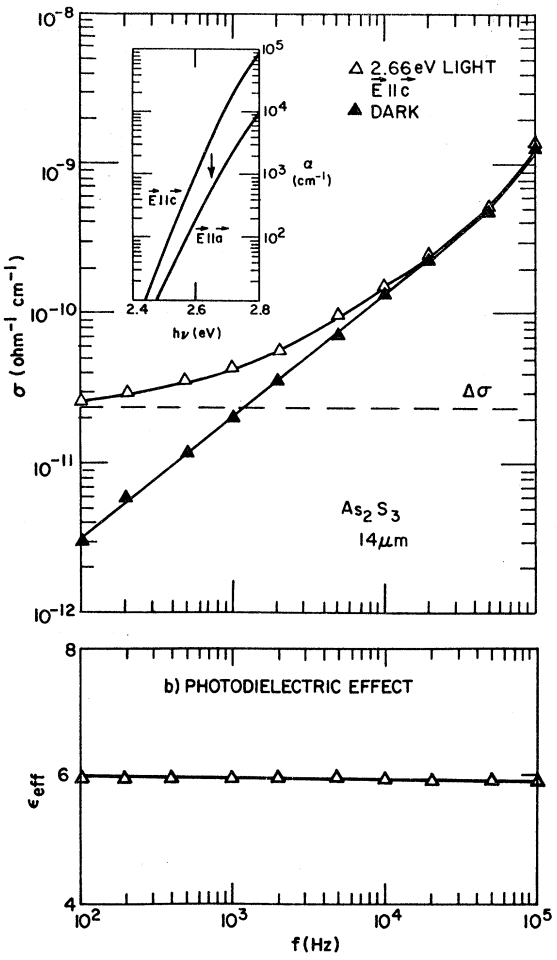

FIG. 3. Dark and photogenerated ac conductivity vs frequency for 14-μm crystal of As_2S_3. Absorption characteristic is shown in insert where arrow indicates excitation energy used. $\Delta\sigma$ is photogenerated increment. Effective dielectric constant vs frequency under illumination is shown in lower part of figure. Photon flux is 10^{15} photons cm^{-2} sec^{-1}. $T=294$°K. Bias 100-mV rms. 1-M saline solution.

photodielectric constant ϵ_{eff}. ϵ_{eff} is nondispersive for the case of uniform light penetration, and is just the true b axis dielectric constant. The light-induced conductivity increment $\Delta\sigma$, represented by the dashed line, is clearly frequency independent over the indicated range. Frequency-independent ac conductivity is characteristic of free carrier dissipation, suggesting that the photoexcited carriers are in extended states. However, in order to determine whether $\Delta\sigma$ reflects the bulk transport parameters of As_2S_3 as well, it is necessary to analyze the role of the electrolytic contacts used in these measurements.[20] At the fields used in making phototransient measurements in As_2S_3, for example, these contacts must be blocking to permit observation of transient signals.[21] Even if we assume that these contacts remain blocking at the very low fields used in the ac experiments, their effect is inconsequential if, on the average, a photoexcited carrier either does not live long enough to encounter the sample boundaries or the ac bias frequency ω is sufficiently high that the condition $\omega t_T > 1$ is satisfied, where t_T is the transit time under $E(\omega)_{rms}$.[20] The assumption of a lifetime limited range is found to be in general accord with experimental observations. If we assume that recombination lifetime limits the range of photoexcited carriers in As_2S_3, then even if the contacts are blocking, we can write

$$\Delta\sigma = e\eta\alpha I(\mu_n\tau_n + \mu_p\tau_p) ,$$

where η is the bulk quantum efficiency under the experimental conditions, α is the absorption coefficient, and I the photon flux. Transient measurements indicate that As_2S_3 is a two-carrier system,[14] and the expression includes microscopic mobilities and recombination lifetimes for both signs of carrier (μ_n, μ_p, τ_n, τ_p). We can extrapolate the bulk quantum efficiency to low fields by fitting a three-dimensional Onsager model for field-dependent photogeneration to the high-field quantum efficiency data. This procedure leads to an estimated quantum efficiency of order 10^{-2}–10^{-1} carriers per absorbed photon.[22] From the data shown in Fig. 3 we estimate for $(\tau_n\mu_n + \tau_p\mu_p)$ $\sim 10^{-8}$–10^{-9} cm^2/V.

Since the rms ac field used in these experiments was typically 10 V/cm and never exceeded 100 V/cm, the observed $\Delta\sigma$ appears to be consistent with the assumed lifetime limitation. In transient measurements it is observed that drift mobilities for electrons and holes are comparable and of order 0.1–1.0 cm^2/V sec.[14] We have no present experimental information from which to determine whether the drift mobility is trap controlled, and can therefore only estimate a nominal upper limit of 100 nsec for the recombination lifetime from the ac data. In the time-of-flight experiment, it was necessary to make the transit time less than 100 nsec to observe a well-defined fiducial point on current traces,[14] suggesting that the deep trapping lifetime is also nominally in the 100-nsec range. The shape of the current transients in crystalline As_2S_3 does not exhibit the dispersive tail characteristic of[23] amorphous As_2Se_3 and some polymer systems. These are systems in which photoexcited carriers are believed to transit by a hopping process. The transients in As_2S_3 closely resemble those observed in amorphous Se,[24,25] where it has been suggested that photoexcited carriers transit the sample in extended states. However, even though carriers in extended states might appear to control both the dissipation under constant illumination measured in the ac experi-

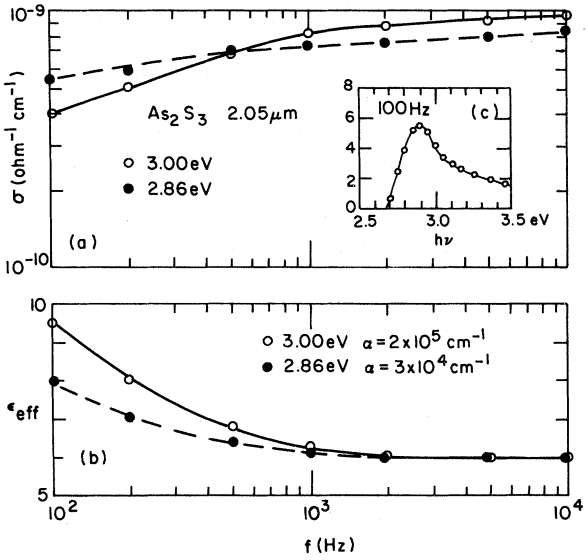

FIG. 4. Photogenerated ac conductivity vs frequency for 3.00-eV irradiation, open circles, and 2.85-eV irradiation, full circles, as measured on a 2.05-μm As_2S_3 single crystal. Normalized spectral dependence of photo effect at 100 Hz is shown on an arbitrary linear scale in insert. Lower part of figure shows corresponding photodielectric effect. Photon flux nominally 10^{15} photons cm^{-2} sec^{-1}. $T = 295$°K. Bias 100 mV rms. 1-M saline solution.

ments and the shape of current transients, these measurements do not sample precisely the same carrier populations. The transient measurement, in particular, selects only those carriers which can individually transit the sample, while the steady-state ac conductivity can reflect contributions from carriers which are severely range limited.

2. *Photogenerated double layer*

Figure 4(a) shows frequency dependence of photogenerated ac conductivity measured in sandwich cell geometry when the exciting monochromatic light is more strongly absorbed in As_2S_3. Absorption coefficients[20] are indicated in Fig. 4(b). The corresponding frequency-dependent photocapacitance expressed as an effective dielectric constant is shown in Fig. 4(b). It is suggested that a dynamic equilibrium is established under steady illumination, which leads to concurrent formation of a dielectric double-layer structure. Current continuity in the steady state requires establishment of an interfacial polarization in a relaxation time determined by the layer dielectric constants, conductivities, and thicknesses. When the ac bias period approaches, and then becomes shorter than, this relaxation time, a characteristic Maxwell-Wagner dispersion is observed.[26] In the 2.05-μm sample for which this effect is illustrated, the onset of this dispersion occurs as frequency decreases below 1 kHz. This type of photogenerated double layer is of interest because in some respects it simulates a contact-insulator interface which is devoid of a number of the familiar complications of a real surface-electrode interaction. We limit ourselves here to two preliminary observations. First, creation of a double layer can occur in any ac experiment measuring spectral dependence of photoconductivity in sandwich geometry, and for this reason the shape of the response curve may depend on the ac bias frequency. Second, the photogenerated ac conductivity and photocapacitance under excitation with nonpenetrating light can also exhibit dc bias field dependence. The normalized spectral dependence of photogenerated ac conductance expressed on a relative linear scale is indicated in the insert of Fig. 4(a) at 100-Hz ac bias frequency. The shape of the spectral dependence curve measured in the ac mode will vary throughout the frequency range of interfacial relaxation. At 100 Hz, for example, Fig. 4(a) shows the photoconductance is greater at 2.86 eV than at 3.00 eV, whereas the reverse is true at 1 kHz. The effect of superimposed dc bias on photogenerated ac conductivity and photocapacitance measured on two As_2S_3 crystal plates whose respective thicknesses vary by about an order of magnitude is shown in Fig. 5. Frequency and amplitude of ac bias are fixed at 100 Hz and 0.1-V rms. White light has been used in this case with the sample acting as its own filter.[19] In the 12.1-μm crystal, a maximum in both photogenerated conductance and capacitance with increasing dc bias is indicated, whereas in the 1.53-μm crystal, these appear to decrease from an initial maximum value and approach constant values with increasing bias. In both cases, with increasing dc bias, the ac conductance tends toward the corresponding dc conductance at that dc bias, while the effective dielectric constant shown in Fig. 5(c) approaches the bulk b-axis dielectric constant measured in the dark. At all values of the dc bias, the light-induced ac-conductivity increment is essentially independent of ac bias frequencies, and exhibits slightly sublinear light intensity dependence.

Similar results have been obtained for several film thicknesses of amorphous selenium using evaporated gold electrodes. Qualitatively similar results are also obtained on As_2S_3 crystals when one uses metallic rather than electrolytic contacts. A maximum in the ac photoconductance and photocapacitance under nonuniform illumination appears at a characteristic dc field which depends on sample thickness, after which both ac conductance and capacitance decrease as dc bias in-

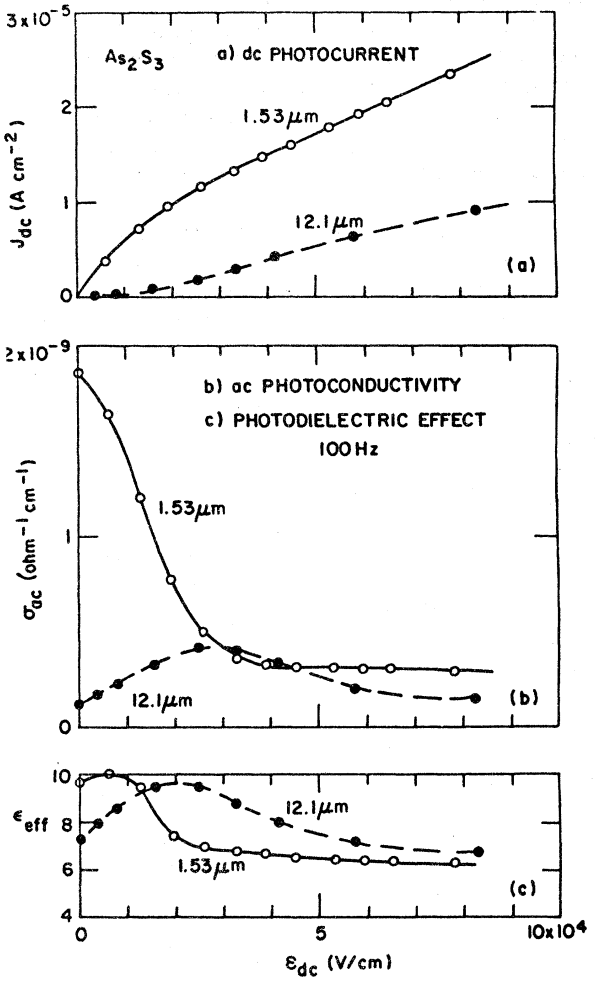

FIG. 5. (a) dc photo current, (b) photogenerated ac conductivity at 100 Hz, and (c) photodielectric effect, vs applied dc field for 1.53 and 12.1-μm As_2S_3 crystals. T = 294 °K. ac bias 100 mV rms. White light photon flux is 5×10^{17} photons cm^{-2} sec^{-1}. 1-M saline solution contacts.

creases. Though these effects are imperfectly understood at present, the following picture is tentatively suggested. Initially, the double-layer structure and the position of the interface are determined principally by the thermal diffusion length of photogenerated carriers. The dc photocurrent is initially controlled by the higher-resistance layer. The effect of dc bias might be to sweep the interface deeper into the crystal bulk and so decrease the resistance of the high-resistance layer. In the simplest ac equavalent circuit for a double layer, which is two parallel RC networks in series, both the equivalent conductance and capacitance would increase initially as the effective resistance of the higher-resistance layer decreased. One extrapolates to a maximum conductance and capacitance as the field entirely eliminates the double layer. The final decrease in conductance and capacitance is more difficult to understand but could reflect the approach to a generation limited condition after space charge has been swept out. In this framework, the approach to a maximum would not be observed in a crystal whose thickness was reduced to the order of a thermal diffusion length (~ 1 μm at 300 °K) and indeed, this seems to be approximately the case when comparing the 1.53- and 12.1-μm crystals. More complete measurements on some amorphous chalcogenides combined with an analysis to establish the factors controlling interface location under bias are planned.

D. Summary and concluding remarks

(i) Frequency-dependent ac conductivity of the form $\sigma = A\omega^s$, $s \leq 1$, a pervasive feature of noncrystalline insulators, is also observed with decreasing temperature in many amorphous semiconductors. There has therefore been speculation that this behavior is fundamentally associated with either long-range positional disorder or an inhomogeneous conductivity effect arising from density fluctuations, both of which are characteristic of amorphous materials. This behavior is now also documented in single crystals of As_2S_3 and anthracene, suggesting instead that it is an experimental feature, common to a large class of solids, which is observed in the absence of stronger loss mechanisms, a common example of which is free-carrier dissipation.

Conductivity of the form $\sigma = A\omega^s$, $s \sim 1$ suggests a distribution of dielectric relaxation times whose width is reflected in the range of experimental frequencies over which this behavior is observed. Measurements in which both temperature and frequency are varied extensively can sometimes distinguish barrier related and a variety of interfacial phenomena, which can also give rise to an apparent frequency-dependent conductivity. One can, in principle, generate barrier models, which would nevertheless predict sublinear frequency-dependent conductivity over a frequency range comparable to that cited in many experimental investigations.[1,10] The possible influence of barriers must therefore always be considered. On the other hand, electronic hopping is known to be the mechanism underlying frequency-dependent conductivity in impurity semiconductors at low temperature.[3,4] Here an experimental connection between dielectric dissipation, the density of hopping sites, and dc impurity conduction is established. In assigning dielectric loss to a charge carrier transport process the limiting connection to dc conductivity is pivotal. For example, in an imagined limit of negligible intersite hopping transport, dielectric dissipation could still arise, in principle, from the spatially

confined motion of charges in a defect or impurity related multivalley local potential. Minimal variation in this potential from site to site could still generate the required relaxation distribution. Resolution of the origin of frequency-dependent conductivity in amorphous solids ultimately remains a materials problem, in that one needs to be able to predictably vary the density of hopping sites. Amorphous Si prepared by the glow discharge of silane is a promising candidate in this respect.[27] Results of a preliminary study of ac conductivity in this system have recently been presented.[28]

(ii) Photogenerated ac conductivity in As_2S_3 using penetrating light (2.66 eV) can be analyzed in terms of bulk transport parameters, providing an average carrier does not encounter the contacts either because of a range limitation or because the excitation frequency is sufficiently high. The use of a quantum efficiency extrapolated to low fields by fitting an Onsager model leads to an estimated $\mu\tau \sim 10^{-8}$–10^{-9} cm^2/V. Comparison with drift mobility data establishes an upper-limit estimate for the recombination lifetime of 100 nsec.

(iii) When the ac conductivity in an As_2S_3 sandwich cell structure is photogenerated using more strongly absorbed light, a characteristic dispersion is generated in both the conductance and capacitance, suggesting a space-charge profile which can be approximately described in terms of a double-layer structure. As a result, there is a range of ac bias frequencies over which the spectral dependence of the normalized photoeffect will appear to vary in shape. Application of superimposed dc field, it is suggested, effects the position of the layer interface, causing the measured conductance and capacitance to vary through a sample-thickness-dependent maximum with increasing dc bias.

ACKNOWLEDGMENTS

We would like to thank Dr. G. Pfister, Dr. H. Scher, Dr. R. Zallen, and Dr. J. Mort for their comments on the manuscript.

[1]See, for example, M. F. Mott and E. A. Davis, *Electro ic Processes in Non-Crystalline Materials* (Clarendon, Oxford, 1971).

[2]J. Tauc, *Amorphous and Liquid Semiconductors* (Plenum, London, 1974).

[3]M. Pollak and T. G. Geballe, Phys. Rev. 122, 1742 (1961).

[4]H. Scher and M. Lax, Phys. Rev. B 7, 4503 (1973).

[5]A. K. Jonscher, *Proceedings of the Fifth International Conference on Amorphous and Liquid Semiconductors*, edited by J. Stuke and W. Brenig (Taylor and Francis, London, 1974).

[6]H. Fritzsche, *Proceedings of the Fourth International Conference on Amorphous and Liquid Semiconductors* edited by J. Stuke and W. Brenig (North-Holland, Amsterdam, 1972).

[7]R. O. Pohl, W. F. Love, and R. B. Stephens, *Proceedings of the Fifth International Conference on Amorphous and Liquid Semiconductors*, edited by J. Stuke and W. Brenig (Taylor and Francis, London, 1974).

[8]U. Strom, J. R. Hendrickson, R. J. Wagner, and P. C. Taylor, Solid State Commun. 15, 1871 (1974).

[9]L. G. Austin and E. S. Garbett, Philos. Mag. 23, 17 (1971).

[10]A. I. Lakatos and M. Abkowitz, Phys. Rev. B 3, 1791 (1971).

[11](a) R. H. Batt, C. L. Braun, and J. F. Hornig, Appl. Opt. Suppl. 3, 20 (1969). (b) F. Guttman and L. F. Lyons, *Organic Semiconductors* (Wiley, New York, 1967); R. S. Berry, J. Jortner, J. C. Mackie, E. S. Pysh, and S. A. Rice, J. Chem. Phys. 42, 1535 (1964); I. M. Dykman, Zh. Eksp. Teor. Fiz. 26, 307 (1954).

[12]H. Scher, D. Pai, and J. Mort, J. Appl. Phys. 44, 2908 (1973).

[13]M. Abkowitz and J. Slowik (unpublished).

[14]D. F. Blossey and R. Enck (unpublished).

[15]See, for example, H. P. Wagner and K. H. Besocke, J. Appl. Phys. 10, 2916 (1969); T. Miyake, *ibid.* 10, 427 (1971); also M. Abkowitz and R. C. Enck (unpublished).

[16]B. L. Evans and P. A. Young, Proc. R. Soc. A 297, 230 (1967).

[17]P. C. Taylor, S. G. Bishop, D. L. Mitchell, and D. Tracey, *Proceedings of the 5th International Conference on Amorphous and Liquid Semiconductors*, edited by J. Stuke and W. Brenig (Taylor and Francis, London, 1974), p. 1267. Also, P. C. Taylor (private communication).

[18]R. Zallen, M. L. Slade, and A. T. Ward, Phys. Rev. B 3, 4257 (1971).

[19]R. Zallen, R. E. Drews, R. L. Emerald, and M. L. Slade, Phys. Rev. Lett. 26, 1564 (1971).

[20]M. Abkowitz, A. I. Lakatos, and H. Scher, Phys. Rev. B 9, 1813 (1974).

[21]W. E. Spear and J. Mort, Proc. Phys. Soc. Lond. 81, 123 (1963). Also, M. Scharfe and F. Schmidlin (private communication).

[22]D. F. Blossey and R. Zallen, Phys. Rev. B 9, 4306 (1974).

[23]H. Scher and E. Montroll (unpublished).

[24]W. E. Spear, Proc. Phys. Soc. Lond. B 70, 669 (1957).

[25]M. D. Tabak, Phys. Rev. 2, 2104 (1970).

[26]See, for example, A. Von Hippel, *Dielectrics and Waves* (Wiley, New York, 1954).

[27]See, for example, Keynote address by W. E. Spear, in *Proceedings of the Fifth International Conference on Amorphous and Liquid Semiconductors*, edited by J. Stuke and W. Brenig (Taylor and Francis, London, 1974), Vol. I, p. 1, and references therein.

[28]M. Abkowitz, P. G. LeComber, and W. E. Spear, Chelsea Conference, December, 1974 (unpublished).